JET-P(94)68

In Situ Determination of the JET Neutral Heating Beam Divergence by Beam Emission Spectroscopy

R C Wolf, D Ciric, R W T König.

JET Joint Undertaking, Abingdon, Oxfordshire, OX14 3EA, UK.

Preprint of a paper to be submitted for publication in
Journal of Applied Physics

December 1994

The spectrum of the Doppler shifted hydrogen Balmer-α emission of the JET neutral heating beams is used to determine their divergence in situ during plasma operation. The line widths have been measured in the presence of the motional Stark effect, employing a numerical fit procedure which makes use of the detailed knowledge of the atomic physics involved. The dependence of the line width on the beam divergence is discussed. The beam divergence is inferred for the various beam operating conditions covering an energy range from 25 to 70 keV/amu and all three hydrogen isotopes. The in situ results are compared to testbed measurements.

I. Introduction

The knowledge of the neutral particle distribution in the neutral heating beams is a precondition for the exact determination of impurity densities by charge exchange recombination spectroscopy (CXRS) [1]. Absolute impurity densities are deduced from the line intensities induced by charge exchange reactions between the beam neutrals and fully ionized bulk plasma ions originating from the cross-over volume between line of sight and beam. This requires the spatial neutral beam particle distribution in the cross-over volume to be known. So far the spatial divergence has been deduced from calorimetric or spectroscopic measurements using testbed facilities [2,3,4]. Using these values for CXRS assumes that the beam properties, like acceleration voltage or focusing, do not change significantly between test and on-line experiment. However, at JET the varying requirements of the tokamak operation make changes of the beam parameters unavoidable, most noticeably the use of tritium [5], for which no testbed measurements are available at all. In this paper it will be shown that the line width of the Doppler shifted Balmer-α beam emission (BE) can be used to determine the neutral beam divergence during plasma operation. The main complication of this method is the presence of a strong magnetic field, which, due to the motional Stark effect (MSE), causes the BE to split into a line multiplet. The advantage is that for any change of beam parameters the divergence can be determined subsequently in situ.

In the presence of a magnetic field **B** a neutral atom moving with a constant velocity **v** experiences in its rest frame a Lorentz electric field $\mathbf{E_L} = \mathbf{v} \times \mathbf{B}$ induced by its own motion. This electric field gives rise to the characteristic splitting of the beam emission (BE) lines. For hydrogen and its isotopes, which exhibit a linear Stark effect, the BE is dominated by the motional Stark effect [6]. The MSE observed on the Balmer-α emission of high energy neutral hydrogen or deuterium beams has been used as a diagnostic for the local magnetic field inside a tokamak plasma [7,8,9,10,11]. Employing a numerical fit procedure developed for the analysis of the Doppler shifted, Stark split BE spectrum, also the line width, which is the quantity containing the information about the beam divergence, can be extracted.

The outline of this paper is as follows: In section II a brief description of the neutral beam configuration and the diagnostic is given in respect to the line width measurement. Section III analyses the various effects leading to a broadening of the BE lines. In the appendix it is shown that the presence of the magnetic field complicates the analyses in so far as the MSE increases the number of lines in the BE spectrum, but the MSE does not contribute significantly to the line broadening. The values of beam divergence, obtained from BE spectroscopy, for the different hydrogen isotopes and a range of beam energies are presented in section IV. They are compared with testbed results in respect to the dependence on energy and beam conditions.

II. Experimental Configuration and Measurement of Line Widths

The JET CXRS and BE diagnostics have been described in detail in earlier papers [12,6]. Here only the components relevant for the understanding of the BE line width measurement will be discussed. Fig. 1 shows the top view of the JET tokamak with the neutral beam injector (NBI) assembly at the torus octant 8, which consists of eight subsytems, so called PINIs (positive ion neutral injector). The eight PINIs are grouped in "normal" and "tangential" banks with a toroidal angle of 7° between them. The four PINIs of each bank are inclined by $\pm 3^{\circ}$ and $\pm 9^{\circ}$ with respect to the torus midplane. Each PINI delivers up to 1.2 MW of neutral particle power. The isotopes hydrogen, deuterium and tritium have been injected into the plasma. The energy for the injected isotopes lie in the range of 25 keV/amu for tritium to 70 keV/amu for hydrogen and deuterium. Each neutral beam consists of three energy fractions corresponding to the presence of H^{+}, H_2^{+} and H_3^{+} in the positive ion source of the neutral beam injector. Construction details of the PINIs result in different 1/e-widths of their density distribution in the horizontal and vertical directions (relative to the beam axis). If x and y denote the horizontal and vertical distance from the axis and d_x and d_y the corresponding 1/e-widths of the beam profile, the shape of the neutral beam profile can be approximated by

$$f \approx e^{-\left(\frac{x}{d_x}\right)^2} e^{-\left(\frac{y}{d_y}\right)^2} . \qquad (1)$$

With z the coordinate along the beam axis, horizontal and vertical beam divergence's are given by

$$d_x = z \tan\varepsilon_x , \qquad (2)$$

$$d_y = z \tan\varepsilon_y . \qquad (3)$$

The JET CXRS and BE diagnostics share the same observation port. An optical head, consisting of a 50 mm lens and a remote controlled mirror, collects light along a set of four, nearly horizontal viewing lines intersecting the axis of the uppermost PINIs of each bank. By moving the mirror the observation positions can be changed radially. The overall range covered, expressed in terms of the angle between viewing line and neutral beam is 45° - 65°. A stack of quartz fibres, located in the focal plane of the lens, is used to relay the light outside the torus hall. There the fibres are imaged onto the entrance slit of a 1.25 m Czerny-Turner spectrometer, which is equipped with a two-dimensional CCD detector recording the spectra from the different viewing lines, and hence different radial positions, simultaneously.

The spectra obtained (fig. 2) are approximated by a sum of Gaussians, convoluted with the instrument function of the spectrometer. The fit of the beam emission spectrum is constrained by enforcing the theoretical symmetry of the Stark features and equidistant spacing in wavelength. In addition, it is assumed that line widths within one energy fraction are constant and that between the different energy fractions they relate to each other like the neutral particle velocity. This assumes a constant neutral beam divergence for the three beam species, which is only approximately valid. Testbed measurements have shown a weak increase of divergence with increasing energy, resulting in a change of the line widths which, however, is small compared to the velocity dependence. The spectral blending of second and third energy components makes it impossible to resolve their line widths independently. Thus the number of free fit parameters is reduced to the number of independent physical parameters required to describe the beam emission spectrum unambiguously [6,11]. By this method, apart from absolute intensities, Doppler shifts and Stark splitting, the line width of the full energy component is determined as a function of radial position. The angle between viewing line and neutral beam, which is an essential parameter in the unambiguous deduction of the beam divergence, is inferred from the Doppler shift of the BE spectrum.

The beam divergence obtained from the in situ measurement is compared to testbed results. The neutral beam testbed diagnostic employs a single viewing line BE diagnostic, intersecting the beam vertically at 52^{o}. Both diagnostics use the same type of spectrometer and CCD detector. The main difference regarding the data analysis is, that in case of the testbed measurement, due to the absence of the magnetic field, the three energy components of the BE spectrum are completely separated.

III. Broadening of the BE spectral lines

In the absence of a magnetic field the various effects contributing to the BE line width [13,14] can be divided into broadening caused by neutral beam and viewing line divergence and by fluctuations of the neutral particle velocity component parallel to the beam axis. Defining an effective neutral beam divergence ε_{eff} (fig. 3), which contains the energy spread of the beam particles perpendicular to the beam axis, the following effects have to be considered [14]:

- Beam focusing: In the JET PINIs the beam particles from a spatially extended source are focused at a point approximately 8 m from the source, leading to an angular velocity distribution along the line of sight.

- Source temperature: A finite source temperature of the order of 1 eV, compared to 80 kV acceleration voltage, gives a divergence of $\approx 0.2^{o}$.

- Dissociation: The dissociation of accelerated molecules and a subsequent transformation of excitation energy into kinetic energy is of the order of a few eV.

- Imperfect acceleration structures also can lead to non-axial velocity components.

Assuming a Gaussian neutral particle distribution the half 1/e-width of the BE line as a function of viewing angle α_0 (angle between line of sight and beam axis) becomes [13,14]

$$\delta_\alpha = \varepsilon_{eff}\, \Delta\lambda_{D,0} \tan \alpha_0 , \qquad (4)$$

where

$$\Delta\lambda_{D,0} = \lambda_0 \frac{v_0}{c} \cos \alpha_0 \qquad (5)$$

is the central Doppler shift (see also Appendix).

Similarly source temperature, dissociation of molecules and imperfect acceleration structures contribute to a spread of the parallel beam velocity. In addition, a ripple of the acceleration voltage has to be taken into account. Expressing the parallel energy spread in terms of

$$\varepsilon_v = \sqrt{\frac{\delta E_v}{E}} , \qquad (6)$$

the contribution to the line width is

$$\delta_v = \varepsilon_v\, \Delta\lambda_{D,0} \; . \qquad (7)$$

It should be noted that $\delta E_v/E$ is the energy variation in the reference frame of the moving beam particles. The corresponding energy variation in the laboratory frame is given by [14]

$$\frac{\delta E_{lab}}{E} = 2\sqrt{\frac{\delta E_v}{E}} . \qquad (8)$$

Finally the effect of a divergent viewing line has to be considered, which is twofold: (A) In the plane of viewing line and beam axis the line broadening is equivalent to the effect of the beam divergence

$$\delta_{vl} = \varepsilon_{vl}\, \Delta\lambda_{D,0} \tan \alpha_0 , \qquad (9)$$

Since the fibres used for the observation of the BE are located in the focal plane of the lens, the acceptance angle ε_{vl} is purely determined by the ratio of fiber diameter to focal length. For the experimental setup used $\varepsilon_{vl} = 0.57^\circ$. (B) In the plane perpendicular to viewing line and beam axis the contribution to the line broadening is of the order [14] $\varepsilon_{vl} / (2 \tan\alpha_0)$ which for $\alpha_0 \approx 60^\circ$ is less than $5 \cdot 10^{-3}$ and therefore can be neglected.

Adding the various broadening effects, under the assumption that they can be approximated by Gaussians, the total 1/e-line width becomes

$$\Delta\lambda_{1/e} = 2\sqrt{\delta_\alpha^2 + \delta_{vl}^2 + \delta_v^2} . \qquad (10)$$

Consequently

$$\Delta\lambda_{1/e} = 2\,\lambda_0 \frac{v_0}{c} \sqrt{(\varepsilon_{eff}^2 + \varepsilon_{vl}^2)\,\sin^2\alpha_0 + \varepsilon_v^2 \cos^2\alpha_0}\ . \qquad (11)$$

Observing the neutral beam at different angles simultaneously, this relation now can be used to determine both the effective beam divergence and the parallel energy spread. It should be noted, that $\Delta\lambda_{1/e}$ depends on the angular beam divergence only, but not on the actual width of the beam along the line of sight, which means it is independent of the location of the beam focus. Due to the near horizontal alignment of the viewing lines ε_{eff} is essentially the horizontal beam divergence.

Since the neutral beam testbed measurement of the line broadening employs a single viewing line only ($\alpha_0 = 52^{o}$) and a single point measurement cannot distinguish between perpendicular and parallel energy spread of the beam neutrals, the apparent beam divergence is introduced for the comparison of in situ with testbed results

$$\varepsilon_{app} \equiv \varepsilon_{eff} \sqrt{1 + \frac{\varepsilon_v^2/\varepsilon_{eff}^2}{\tan^2\alpha_0}}\ . \qquad (12)$$

Obviously ε_{app} is larger than ε_{eff} depending on the ratio $\varepsilon_v/\varepsilon_{eff}$. Because of the vertical alignment of the viewing line ε_{eff} used here represents the vertical beam divergence. Using the definition of ε_{app} the total 1/e-line width becomes

$$\Delta\lambda_{1/e} = 2\,\lambda_0 \frac{v_0}{c}\ \sin\alpha_0 \sqrt{\varepsilon_{app}^2 + \varepsilon_{vl}^2}\ . \qquad (13)$$

In contrast to the in situ measurement, the testbed measurement can resolve the three energy fractions sufficiently, due to the absence of the magnetic field, and hence determine the change of ε_{app} with beam species.

So far the line broadening due to the MSE has not been taken into account. Compared to the Doppler shift, which changes along the line of sight according to the viewing angle and neutral particle velocity distribution, for the variation of the Stark splitting, given by $|\mathbf{v} \times \mathbf{B}|$, also the magnetic field distribution has to be considered. Since the Stark splitting is zero for the central 0σ-line and increases in discrete steps for the other lines, the broadening changes for the different Stark lines. An estimate of the line broadening due to MSE (see Appendix) shows that under the present experimental conditions it can be neglected compared to the effect of the Doppler shift. This is supported by the experimental evidence, which shows constant line widths within each energy fraction.

IV. Determination of Beam Divergence

The BE line widths as a function of viewing angle have been measured for the three hydrogen isotopes, hydrogen, deuterium and tritium. The energy regions investigated are the low voltage (≈ 80 kV), high current and the high voltage (≈ 140 kV), low current configurations at approximately the same levels of injected neutral beam power (≈ 1 MW per PINI).

In fig. 4 the results for two JET discharges with deuterium neutral beam injection at 40.0 keV/amu (#26182) and 68.9 keV/amu (#24738) are presented. Equ. (11), which describes the dependence of the line width on the viewing angle, is employed to fit the measured data points. They represent the average taken over the NBI heating period. The off-set of the two curves reflects the overall energy dependence of the line widths. The effective beam divergence, obtained from the fit of a range of neutral beam configurations and selected from 1500 JET discharges with octant 8 NBI, is shown in fig. 5.. The divergence for hydrogen and deuterium beams lies between 0.59° and 0.72° and shows neither a clear dependence on the isotope used, nor on the beam energy, nor on the PINI used. The observed scatter of the data, however, is bigger than the individual errors, which points to variations in the neutral beam configuration with time. Only the tritium beam at 26.0 keV gives a significantly higher divergence of 0.86°.

The second parameter, obtained from the fit of the line widths, is the parallel energy spread ε_v of the neutral particles in their rest frame. Transformed into the laboratory system it is of the order of $\delta E_{lab}/E \approx 0.01$. Since the measurements are performed at viewing angles closer to 90° than to 0° and ε_v is smaller than ε_{eff}, the relative error of $\delta E_{lab}/E$ is close to $\pm 100\%$. The same argument, however, explains the much smaller uncertainty in the determination of the beam divergence ($\approx \pm 0.05^{\circ}$, which is less than 10%).

The energy dependence of the apparent divergence for the full energy component of a deuterium neutral beam measured in the neutral beam testbed is shown in fig. 6. Similar to the in situ results (fig. 5), for the energy range between 30 and 80 keV/amu no obvious change with energy is observed. The rise of ε_{app} at lower energies can be attributed to space charge effects in the accelerator region (prior to neutralization), and to non-optimal focusing properties of the accelerating structure at low extraction voltages. The scattering of the data in fig. 6 can be explained by non-optimal ion source conditions. In the course of the measurement shown in fig 6 the minimum beam divergence has been adjusted only at a few points by optimizing the ion source parameters to perveance match conditions (see below).

The absolute values of beam divergence shown in figs. 5 and 6 differ by $\approx 0.3^{\circ}$. As already indicated in section III, this can be explained by the difference between horizontal and vertical beam divergence, and the use of ε_{app} instead of ε_{eff}. In both cases the divergence from testbed measurements is expected to be larger than from in situ measurements. The testbed measurements have been performed with the viewing line in the vertical plane and calorimetric measurements of the beam profile suggest that the vertical divergence is equal or slightly larger than the horizontal divergence. In addition, ε_{app} includes both the parallel and the perpendicular energy spread which yields larger values compared to ε_{eff}.

The variation of the apparent beam divergence for the three components of the deuterium beam with beam perveance at fixed acceleration voltage of 132 kV is shown in fig. 7. Perveance is defined as the ratio between extracted beam current and the extraction voltage to the power of 3/2 ($I_{ex}/U_{ex}^{3/2}$) and is commonly used to characterize high power particle beam sources. In practice, the optimum beam conditions (i.e. minimum beam profile width, minimum beam divergence, maximum beam transmission) are found by varying the arc current of the PINI ion source at fixed extraction voltage. The minimum beam divergence corresponds to so called perveance match conditions. The optimum perveance is the characteristics of the ion source, and varies for different ion sources.

During neutral beam injection into JET, the requirement is to operate different ion sources at the corresponding perveance match conditions. In practice, due to slightly different power supply set points and small variations in ion source gas pressures, beams are injected at conditions close to perveance match. This could explain the scattering of the in situ beam divergence data shown in fig. 5. Particularly, in the case of the tritium beam, the source was not operated at the perveance match condition. Due to a limited amount of tritium gas used in the JET preliminary tritium experiment [5], the gas pressure of the tritium ion source was lower than the nominal one. To provide a reliable ion source operation at this low pressure, the beam current was set to a value different from perveance match condition. This explains the higher beam divergence of the tritium beam compared to hydrogen or deuterium.

Also seen in fig. 7 is the variation of the beam divergence for the three energy fractions. The corresponding change of the line width compared to the dependence of the line width on the beam energy is only 10 to 15%. This justifies that the coupling of the line widths of the half and third energy component to the width of the full energy component in the fit procedure of the Stark multiplet neglects the change of the beam divergence with beam species, also considering the line blending within half and third energy fractions.

V. Summary and Conclusions

It has been shown that BE spectroscopy during plasma operation, measuring the fully resolved Stark spectrum, is a feasible method for the determination of the neutral heating beam divergence. Employing a numerical fit procedure to extract the line widths of the full energy component, the dependence of the line width on the viewing angle is used to infer both parallel and perpendicular energy spread of the neutral beam particles. Here the motional Stark effect complicates the structure of the BE spectrum, but in itself does not contribute to the broadening of the BE lines significantly.

The comparison of in situ with testbed results shows good agreement in terms of the energy dependence of the beam divergence. The small deviations observed for the absolute values can be explained by the difference between vertical and horizontal divergence and the fact that the testbed measurement cannot distinguish between parallel and perpendicular energy spread of the beam particles. In situ measurements have been performed on all three hydrogen isotopes, including tritium. The higher divergence of the tritium beam is explained by non-optimized perveance match conditions required by a reduced pressure in the ion source.

The results presented here are of particular importance for CXRS, which for the deduction of impurity densities relies on the exact knowledge of the spatial distribution of the beam neutrals along the line of sight. Provided CXRS and BE spectroscopy share the same viewing lines crossing the neutral beam axis, the measured divergence can be directly used for deduction of the impurity density by CXRS, disregarding whether the measured ε_{eff} is a composition of horizontal and vertical beam divergence. In case the operating conditions of the beams such as energy and beam species are changed frequently, variations of the divergence have to be expected. Therefore an in situ determination of the divergence provides an ideal tool for the examination of the beam divergence which subsequently can be used for CXRS.

Appendix

Estimate of line broadening due to MSE

In order to estimate the contributions of the various effects to the final line width, the approach of Ott et al. [14] is used, which calculates small deviations in form of differentials around a central Doppler shift or Stark splitting. The broadening of the BE lines due to Doppler and Stark effects will be referred to as Doppler and Stark broadening. The Doppler broadening depends on the angular velocity distribution along the line of sight and the energy spread parallel to the beam axis and is constant for all lines within one energy fraction of the Stark spectrum. In addition, the Stark broadening also depends on the magnetic field distribution. In contrast to the Doppler shift the Stark splitting is zero for the central 0σ-line and increases in steps of $\Delta e = 1,2,3,4$ for the 1σ, 2π, 3π, 4π components respectively. Hence the contribution to the line broadening changes within one energy fraction.

The Doppler shift of a spectral line λ_0 emitted by beam particles at a viewing angle α with respect to the beam velocity v (fig. 3) is given by

$$\Delta\lambda_D = \lambda_0 \frac{v}{c} \cos\alpha , \qquad \text{(A.1)}$$

where here $\lambda_0 = 6561$ Å is the D_α-wavelength. For velocities of the order $v/c \approx 0.01$ the non-relativistic approximation of the Doppler shift can be used. The contributions to the Doppler broadening as a result of a deviation from the central Doppler shift

$$\Delta\lambda_{D,0} = \lambda_0 \frac{v_0}{c} \cos\alpha_0 \qquad \text{(A.2)}$$

due to a distribution of α and v become

$$\delta_{\alpha,D} \equiv \frac{d(\Delta\lambda_D)}{d\alpha} d\alpha = -\Delta\lambda_{D,0} \tan\alpha_0 \, d\alpha , \qquad \text{(A.3)}$$

$$\delta_{v,D} \equiv \frac{d(\Delta\lambda_D)}{dv} dv = \Delta\lambda_{D,0} \frac{dv}{v_0} . \qquad \text{(A.4)}$$

It should be noted, that dv is the variation of the parallel velocity, whereas the variation of the perpendicular velocity is contained in $d\alpha$ (parallel and perpendicular to the beam axis). The Stark splitting is determined by the electric field $E_L = |\mathbf{v} \times \mathbf{B}| = v B \sin\beta$ (fig. 8) and, expressed in terms of a wavelength shift relative to the central 0σ-component, is

$$\Delta\lambda_S = \frac{3}{2}\,\frac{e\,a_0}{h\,c}\,\lambda_0^2\,\Delta e\,v\,B\,\sin\beta\,, \qquad (A.5)$$

where e is the electron charge, a_0 the Bohr radius and h the Planck constant. Analogous to the Doppler broadening, the Stark broadening can be estimated by calculating the deviations from a central splitting

$$\Delta\lambda_{S,0} = \frac{3}{2}\,\frac{e\,a_0}{h\,c}\,\lambda_0^2\,\Delta e\,v_0\,B_0\,\sin\beta_0\,. \qquad (A.6)$$

For the Stark broadening the following contributions have to be considered: (A) With a variation of α the angle β between the magnetic field orientation and the neutral particle velocity changes. By expressing β as a function of the viewing line coordinate s and s as a function of α, this leads

$$\delta_{\alpha,S1} \equiv \left.\frac{d(\Delta\lambda_S)}{d\alpha}\right|_{B=\mathrm{const}} d\alpha \approx \frac{\Delta\lambda_{S,0}}{\sin\alpha_0\,\tan\beta_0}\,d\alpha\,, \qquad (A.7)$$

already taking into account that the distance between observation position and beam focus $z_0 \ll R_\perp$. (B) The second contribution comes from a variation of $B \sim 1/R$ along the viewing line (the poloidal magnetic field is neglected). Similar to (A) the differential is calculated by expressing B as a function of s and s as a function of α:

$$\delta_{\alpha,S2} \equiv \left.\frac{d(\Delta\lambda_S)}{d\alpha}\right|_{\beta=\mathrm{const}} d\alpha = \frac{\Delta\lambda_{S,0}}{\sin\alpha_0}\,\frac{s_\perp z_0}{R_0^2}\,d\alpha\,. \qquad (A.8)$$

(C) Finally, the distribution of v gives

$$\delta_{v,S} \equiv \frac{d(\Delta\lambda_S)}{dv}\,dv = \Delta\lambda_{S,0}\,\frac{dv}{v_0}\,. \qquad (A.9)$$

In order to compare Stark and Doppler broadening the maximum Stark broadening, experienced by the outermost components ($\Delta e = 4$), is used. For typical experimental values ($v_0 = 3\cdot 10^6$ m/s, $\alpha_0 = 60^\circ$, $B_0 = 2.5$ T, $\beta_0 = 70^\circ$) the central Doppler shift and Stark splitting are

$$\Delta\lambda_{D,0} \approx 33\ \text{Å}\,,$$
$$\Delta\lambda_{S,0} \approx 8\ \text{Å}\,.$$

Finally, the contributions to the line width become

Stark broadening:	Doppler broadening:
$\delta_{\alpha,S1} \approx 3\ \text{Å}\,d\alpha$	$\delta_{\alpha,D} \approx 57\ \text{Å}\,d\alpha$
$\delta_{\alpha,S2} \approx 0.5\ \text{Å}\,d\alpha$	
$\delta_{v,S} \approx 8\ \text{Å}\,\frac{dv}{v_0}$	$\delta_{v,D} \approx 33\ \text{Å}\,\frac{dv}{v_0}\,.$

Comparing the corresponding terms, it can be concluded that the Stark broadening, under the experimental conditions presented here, is negligible.

Acknowledgments

The authors would like to thank the continuos support and encouragement of P. R. Thomas. They also wish to thank M. von Hellermann for his constant interest in the subject of this paper and H. Falter for very helpful discussions on physics of the neutral heating beams.

References

[1] M. G. Hellermann, H. P. Summers, Atomic and Plasma-Material Interaction Processes in Controlled Thermonuclear Fusion, R. K. Janev and H. W. Drawin (editors), 1993 Elsevier Science Publishers B. V.

[2] C. F. Burell, W. S. Cooper, R. R. Smith, W. F. Steele, Rev. Sci. Instr. **51**, 1451 (1980)

[3] J. F. Bonnal, G. Bracco, C. Breton, C. de Michelis, J. Druaux, M. Mattioli, R. Oberson, J. Ramette, J. Phys. D: Appl. Phys. **15**, 805 (1982)

[4] H. W. Kugel, G. M. Gammel, L. R. Grisham, R. Kaita, J. H. Kamperschroer, R. A. Langley, C. W. Magee, S. S. Medley, T. J. Murphy, A. L. Roquemore, M. D. Williams, Rev. Sci. Instr. **60**, 37 (1988)

[5] The Jet Team, Nucl. Fus. **32**, 187 (1992)

[6] W. Mandl, R. C. Wolf, H. P. Summers, M. von Hellermann, Plasma Phys. Control. Fusion **35**, 1373 (1993)

[7] F. M. Levinton, R. J. Fonck, G. M. Gammel, R. Kaita, W. Kugel, E. T. Powell, D. W. Roberts, Phys. Rev. Lett **63**, 2060 (1989)

[8] F. M. Levinton, Rev. Sci. Instr. **63**, 5157 (1992)

[9] D. Wróblewski, L. L. Lao, Rev. Sci. Instr. **63**, 5140 (1992)

[10] R. C. Wolf, J. O'Rourke, A. W. Edwards, M. von Hellermann, Nucl. Fus. Lett. **33**, 663 (1993)

[11] R. C. Wolf, L.-G. Eriksson, M. von Hellermann, R. König, W. Mandl, F. Porcelli, Nucl. Fus. 33, 1835 (1993)

[12] M. von Hellermann, W. Mandl, H. P. Summers, H. Weisen, A. Boilau, P. Morgan, H. Morsi, R. König, M. F. Stamp, R. C. Wolf, Rev. Sci. Instr. **61**, 3479 (1990)

[13] G. Bracco, C. Breton, C. de Michelis, M. Mattioli, J. Ramette, J. Opt. Soc. Am. **71**, 1318 (1981)

[14] W. Ott, F.-P. Penningsfeld, Report IPP 4/258, Max-Planck-Institut für Plasmaphysik, D-8046 Garching (1993)

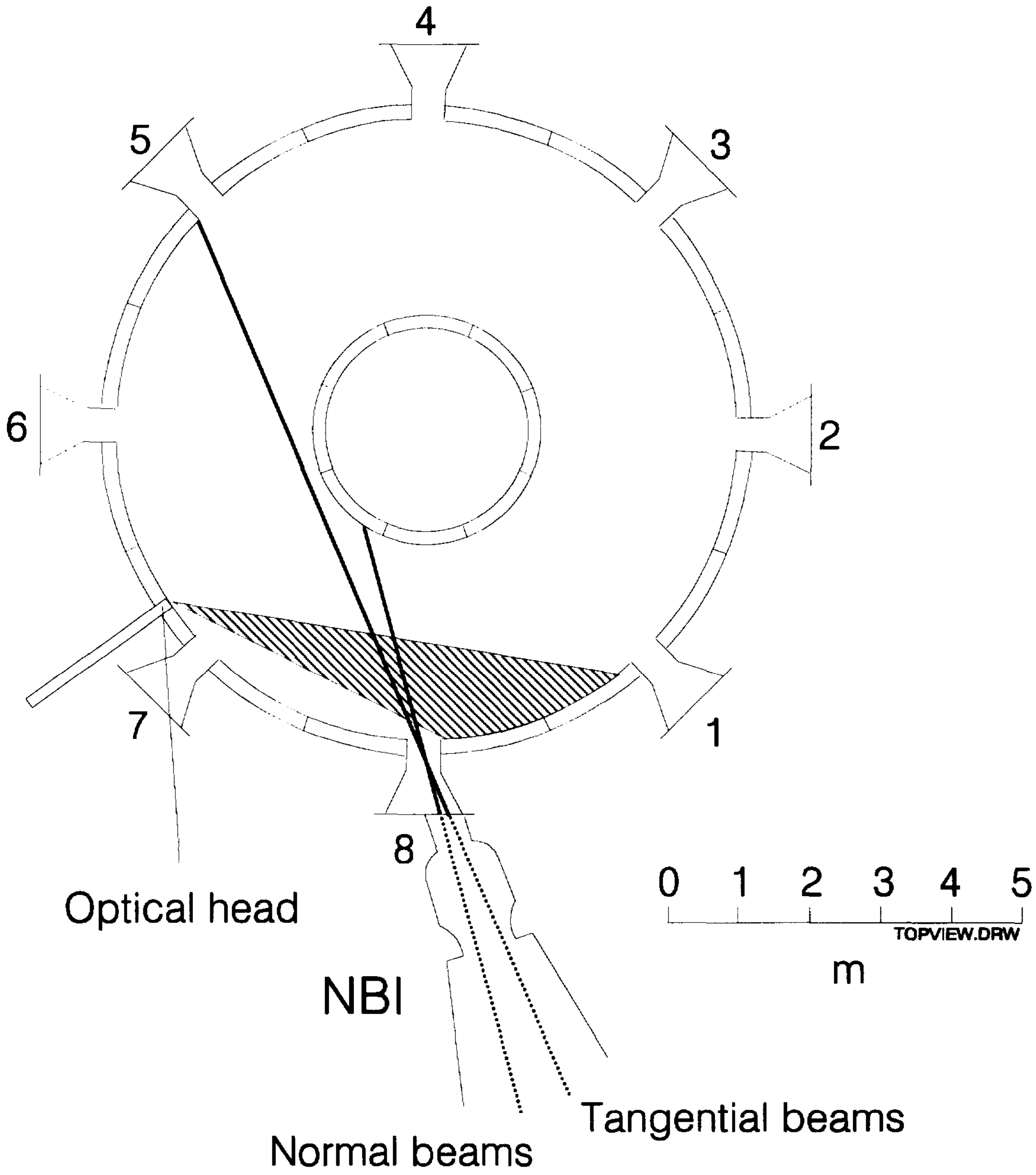

Fig. 1. Top view of the JET tokamak showing the neutral beam injector assembly at the torus octant 8. An optical head collects light along a set of four, nearly horizontal viewing lines intersecting the axis of the uppermost PINIs of each bank.

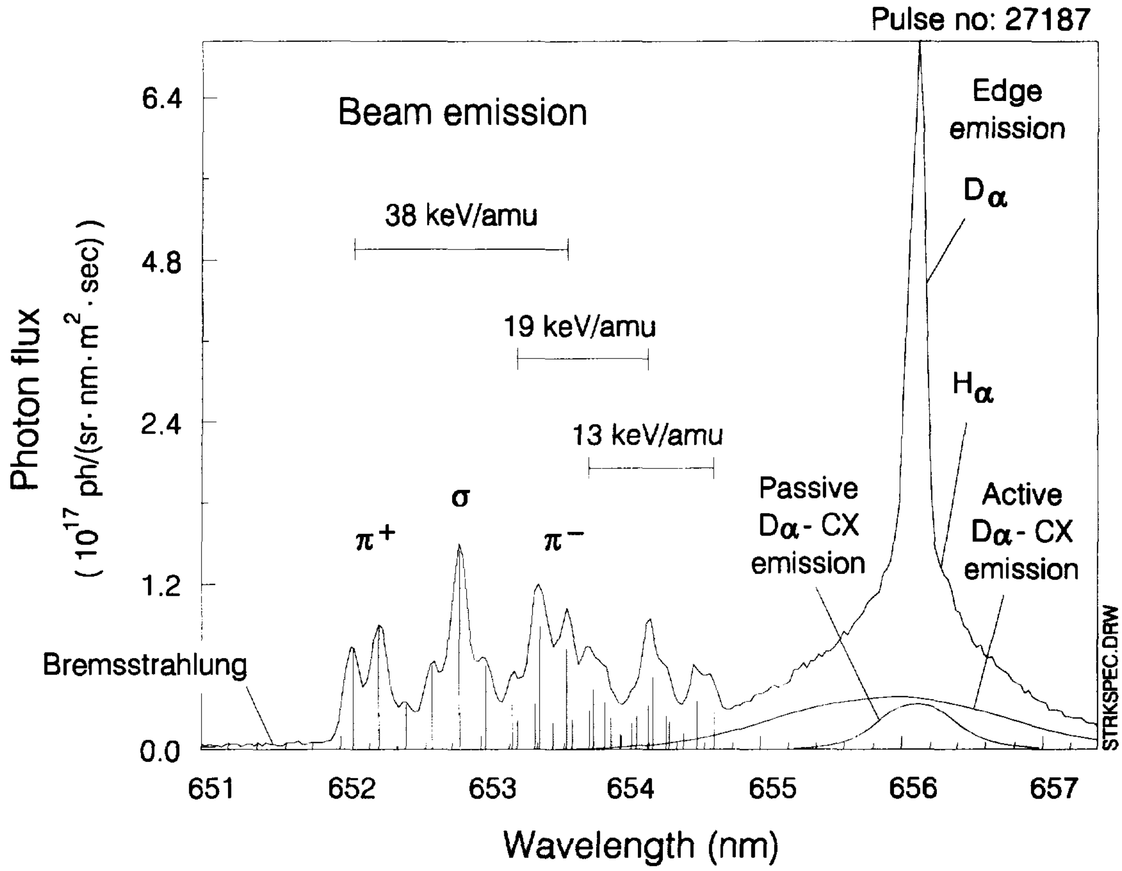

Fig. 2. D_α spectrum consisting of edge emission, charge exchange (CX) emission and Doppler-shifted beam emission. The beam emission consists of three energy components. The positions of the individual Stark line are indicated by vertical bars.

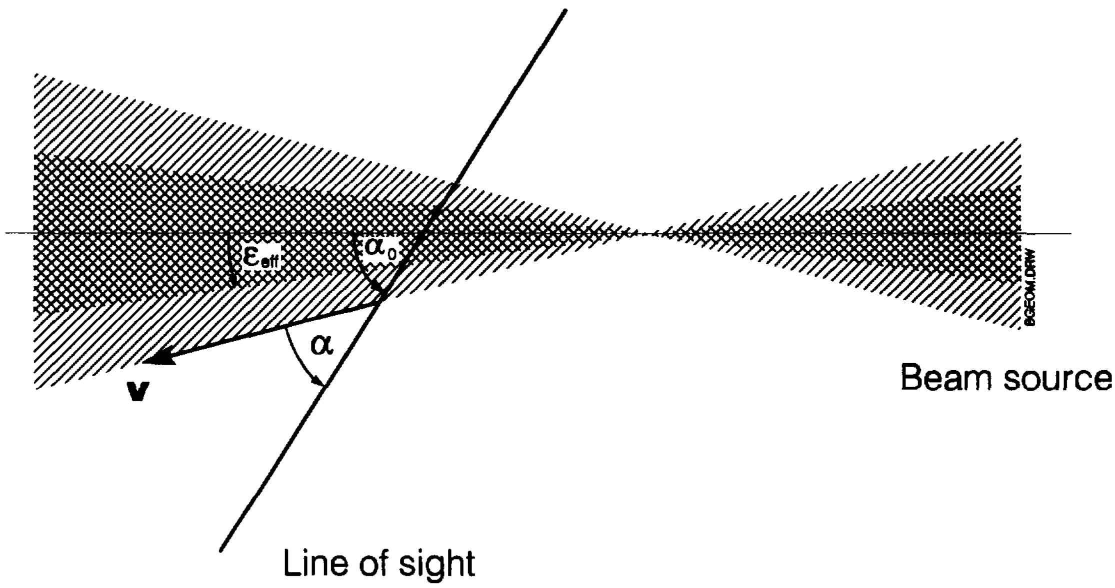

Fig. 3. Beam and viewing geometry. The plane of beam axis and line of sight is approximately parallel to the torus midplane. The beam divergence, typically 0.5° - 1.0° is not drawn to scale.

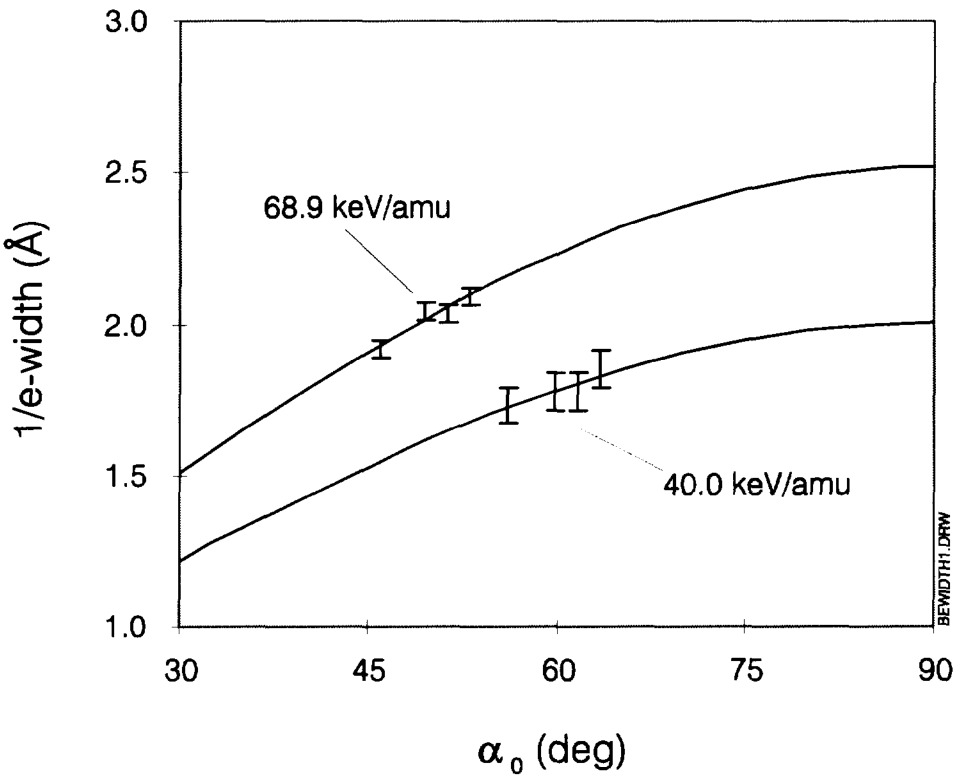

Fig. 4. Full 1/e-width of the full energy component vs viewing angle. The measured data and the corresponding fits of equ. (11) (solid lines) for two NBI heated discharges with different beam energies are compared. The error bars represent the variation of the measured data during the NBI heating period.